Less Invasive Phenotype Found in Isocitrate Dehydrogenase–mutated Glioblastomas than in Isocitrate Dehydrogenase Wild-Type Glioblastomas: A Diffusion-Tensor Imaging Study[1]

Stephen J. Price, PhD, FRCS
Kieren Allinson, FRCPath
Hongxiang Liu, PhD, FRCPath
Natalie R. Boonzaier, PhD
Jiun-Lin Yan, MD[2]
Victoria C. Lupson, BS
Timothy J. Larkin, PhD

Purpose: To explore the diffusion-tensor (DT) imaging–defined invasive phenotypes of both isocitrate dehydrogenase (IDH-1)–mutated and IDH-1 wild-type glioblastomas.

Materials and Methods: Seventy patients with glioblastoma were prospectively recruited and imaged preoperatively. All patients provided signed consent, and the local research ethics committee approved the study. Patients underwent surgical resection, and tumor samples underwent immunohistochemistry for IDH-1 R132H mutations. DT imaging data were coregistered to the anatomic magnetic resonance study and reconstructed to provide the anisotropic and isotropic components of the DT. The invasive phenotype was determined by using previously published criteria and correlated with IDH-1 mutation status by using the Freeman-Halton extension of the Fisher exact probability test.

Results: Nine patients had an IDH-1 mutation and 61 had IDH-1 wild type. All of the patients with IDH-1 mutation had a minimally invasive DT imaging phenotype. Among the IDH-1 wild-type tumors, 42 of 61 (69%) were diffusively invasive glioblastomas, 14 of 61 (23%) were locally invasive, and five of 61 (8%) were minimally invasive ($P < .001$).

Conclusion: IDH-mutated glioblastomas have a less invasive phenotype compared with IDH wild type. This finding may have implications for individualizing the extent of surgical resection and radiation therapy volumes.

[1] From the Cambridge Brain Tumour Imaging Laboratory, Division of Neurosurgery (S.J.P., N.R.B., J.L.Y., T.J.L.), and Wolfson Brain Imaging Centre, Department of Clinical Neurosciences (S.J.P., N.R.B., V.C.L., T.J.L.), University of Cambridge, Cambridge Biomedical Campus, Cambridge CB2 0QQ, England; and Department of Histopathology (H.L.) and Molecular Malignancy Laboratory (K.A., H.L.), Addenbrooke's Hospital, Cambridge, England. Received December 5, 2015; revision requested February 8, 2016; revision received July 17; accepted August 12; final version accepted September 7. **Address correspondence to** S.J.P. (e-mail: sjp58@cam.ac.uk).

S.J.P. supported by NIHR Clinician Scientist Fellowship (NIHR/CS/009/011). J.L.Y. supported by a grant from the Chang Gung Medical Foundation and Chang Gung Memorial Hospital. N.R.B. supported by a grant from the Commonwealth Scholarship Commission and Cambridge Commonwealth Overseas Trust. The Human Research Tissue Bank is supported by the NIHR Cambridge Biomedical Research Centre.

This paper presents independent research funded by the National Institute for Health Research (NIHR). The views expressed are those of the authors and not necessarily those of the NHS, the NIHR, or the Department of Health.

Current address:
[2] Department of Neurosurgery, Chang-Gung University and Memorial Hospital, No. 222, Maijin Rd, Anle District, Keelung City, Taiwan 204, Keelung, Taiwan.

Glioblastoma is the most common and most aggressive primary tumor of the brain and is associated with an appalling prognosis. Recent developments in molecular biology challenged the traditional classification of glioblastoma on the basis of features observed with light microscopy, with a subclassification on the basis of molecular markers. The discovery of mutations of the isocitrate dehydrogenase (IDH) gene, an early event in the development of low-grade gliomas (1), led to the realization that some glioblastomas have this mutation (2–4). Nearly 90% of IDH mutations that affect both the cytostolic form IDH, IDH-1, and, less commonly, the mitochondrial form, IDH-2, are point mutations (1,2), which are detected with immunohistochemistry (5).

Patients with glioblastoma and IDH mutations have a better prognosis; their median survival is 31 months, compared with 15 months in patients with IDH wild type (3,6). The reason that mutations of IDH improve survival is not fully understood. Normally functioning IDH appears to be important in protecting cells against the oxidative stress caused by radiation therapy or chemotherapy. Therefore, mutations of IDH may increase sensitivity to cellular damage caused by radiation therapy and chemotherapy. This does not, however, explain findings by Beiko et al (7), who demonstrated that complete resection of the enhanced tumor leads to better survival in IDH-mutated compared with IDH wild-type glioblastomas. The outcome was even better in the mutant group when the resection extended into the nonenhanced tumor. These findings suggest differences in the invasive behavior of IDH-mutated tumors.

Advance in Knowledge

- This study of nine patients with glioblastoma and isocitrate dehydrogenase (IDH) mutations (nine of 70 [13%]) showed that the nine glioblastomas with IDH mutations appeared to have a diffusion-tensor imaging–defined, minimally invasive phenotype.

Invasion of glioma cells into the surrounding healthy brain is a cardinal feature of glioblastoma and is a major cause of our failure to achieve local control. This occult invasion cannot be identified at conventional anatomic magnetic resonance (MR) imaging (8–10) and therefore has been difficult to study. Because the invasion primarily involves white matter tracts, the use of diffusion-tensor (DT) imaging to help to identify this white matter disruption has been investigated as a suitable imaging marker of invasion. DT imaging depicts differences in the peritumoral region of invasive gliomas that are not found in noninvasive meningiomas or metastases (11,12). Specimens from image-guided biopsies of these regions showed that DT imaging can accurately depict tumor invasion (10,13) and can be used to predict the pattern of tumor progression (14). These DT imaging–defined invasive regions undergo perfusion and spectroscopic changes that resemble tumor (15). Through use of these methods, it is clear that about 20% of tumors have what has been described as a minimally invasive DT imaging phenotype (14), and these tumors have a longer time to progression (16).

We hypothesized that IDH-mutated glioblastomas will have DT imaging features that suggest a less invasive phenotype than that observed in IDH wild-type glioblastomas. This study sought to explore the DT imaging–defined invasive phenotypes of both IDH-mutated and IDH wild-type glioblastomas.

Materials and Methods

Patients

Seventy patients with glioblastoma confirmed with histologic analysis were prospectively recruited to this study between August 2011 and October 2014. All patients were approached if they had a good performance status (World Health Organization performance status 0–1) and a tumor that the operating neurosurgeon indicated was suitable for a maximal resection assisted by 5-aminolevulinic acid fluorescence guidance (17). Patients with metallic implants not compatible with MR imaging (two patients) or those who were severely claustrophobic (five patients) were excluded. Only two patients who were approached declined to take part in this study. All patients provided signed consent, and the local research ethics committee approved the study.

MR Imaging Studies

Before surgery, patients underwent imaging with a 3-T MR imager (Magnetom Trio; Siemens Healthcare, Erlangen, Germany) by using a standard 12-channel receive-head coil and transmission on the body coil. Imaging sequences included conventional anatomic imaging sequences and DT imaging. The anatomic sequences included the following: an axial precontrast T1-weighted sequence (repetition time [msec]/echo time [msec]: 500/8.6; number of signals acquired, one; section thickness, 4 mm; intersection gap, 1 mm; in-plane resolution, 0.74 mm; field of view, 24 × 24 cm; and imaging time, 4 minutes

Implication for Patient Care

- This study helped to improve understanding of the better prognosis of IDH-mutated glioblastomas, and it may have future implications for individualizing the extent of surgical resection and radiation therapy volumes.

Published online before print
10.1148/radiol.2016152679 **Content code:** NR

Radiology 2017; 000:1–7

Abbreviations:
DT = diffusion tensor
IDH = isocitrate dehydrogenase

Author contributions:
Guarantor of integrity of entire study, S.J.P.; study concepts/study design or data acquisition or data analysis/interpretation, all authors; manuscript drafting or manuscript revision for important intellectual content, all authors; approval of final version of submitted manuscript, all authors; agrees to ensure any questions related to the work are appropriately resolved, all authors; literature research, S.J.P., H.L.; clinical studies, S.J.P., J.L.Y., V.C.L.; statistical analysis, S.J.P.; and manuscript editing, S.J.P., K.A., H.L., N.R.B., T.J.L.

Conflicts of interest are listed at the end of this article.

22 seconds); an axial fluid-attenuated inversion recovery sequence (7840/95; inversion time, 2500 msec; number of signals acquired, one; section thickness, 4 mm; intersection gap, 1 mm; in-plane resolution, 0.7 mm; field of view, 22.4 × 16.8 cm; imaging time, 4 minutes 28 seconds). DT imaging was performed with a single-shot spin-echo echo-planar imaging sequence (8300/98 msec; section thickness, 2 mm; no gap; in-plane resolution, 2 mm [providing isotropic voxel size to allow three-dimensional appreciation of white matter]; 12 directions; *b* values: 350, 650, 1000, 1300, and 1600 sec/mm^2; field of view, 19.2 × 19.2 cm; and imaging time, 9 minutes 26 seconds).

After intravenous injection of 9 mL of gadobutrol (Gadovist, 1.0 mmol/mL; Bayer, Leverkusen, Germany) followed by a 20-mL saline flush, a three-dimensional T1-weighted inversion recovery sequence was performed (magnetization-prepared rapid gradient echo; 2300/2.98; inversion time, 900 msec; number of signals acquired, one; section thickness; 1 mm; no gap; in-plane resolution, 1 mm; field of view, 25.6 × 24.1 cm; and imaging time, 9 minutes 14 seconds).

Imaging Data Postprocessing

We performed data processing offline. DT imaging data were processed by using the FDT toolbox in FSL (FMRIB software; Oxford Centre for Functional MR Imaging of the Brain, Oxford, England). For each voxel, the eigenvalues (λ_1, λ_2, and λ_3) were calculated and were used to construct fractional anisotropy and p and q maps by using the previously described methods and terminology (18). For each of the p and q maps, regions of interest were drawn by using software (ImageJ; National Institutes of Health, Bethesda, Md) around the visible region of increased isotropic diffusion (for the p abnormality) and decreased anisotropic diffusion (for the q abnormality) by a neurosurgeon (S.J.P.) with 15 years of experience outlining these abnormalities. This neurosurgeon was blinded to the IDH mutation status. Previous work (15) showed that this method has good intra- and interrater agreement.

One author (S.J.P., with 16 years of experience with DT imaging data and image analysis) classified the invasive phenotype by using a modification of previously published classification system (14). Three invasive phenotypes were identified on the basis of the following DT imaging data: *(a)* diffuse invasive phenotype, if the p abnormality exceeded the q abnormality by more than 1 cm in all directions (a distance used in previous postmortem studies [19,20]); *(b)* localized invasive phenotype, if the p abnormality exceeded the q abnormality by more than 1 cm in one particular direction; and *(c)* minimal invasive phenotype, if the p abnormality was similar to the q abnormality.

To confirm that changes in adjacent white matter tracts show invasion, small-point regions of interest were placed in the white matter adjacent to the tumor, as determined by the fractional anisotropic maps. Measurements of p and q were performed and the tissue signature plotted with the p value on the x-axis and the q value on the y-axis by using previously published methods (21). Examples are shown in Figures 1 and 2. On the basis of previously published studies, an increase of greater than 10% compared with contralateral white matter for the isotropic (p) component and a reduction of greater than 12% compared with contralateral white matter were considered statistically significantly different (10,21).

Pathologic Assessment and IDH-1 R132H Immunohistochemistry

All patients underwent surgical resection of the tumor with the intention to maximally resect the tumor. Tumor samples were fixed in 10% formalin and embedded in paraffin wax. Slices that were 4–μm thick were cut and stained with hematoxylin and eosin for light microscopy. The diagnosis of glioblastoma was on the basis of the World Health Organization 2007 histopathologic criteria: an infiltrative astrocytic neoplasm with high proliferative activity and microvascular proliferation, necrosis, or both (22).

Immunohistochemistry was performed on slices in which the paraffin was removed, after heat-induced antigen retrieval, to evaluate the presence or absence of the IDH-1 R132H mutation. Mutation-specific antibodies (Dianova, Hamburg, Germany) were used at a 1:20 dilution and were viewed by using a secondary antibody avidin-based detection system. Cytoplasmic immunoreactivity was regarded as a positive reaction. Negative and positive control tissues were stained appropriately.

IDH Sequencing

In five patients who did not have an IDH-1 R132H mutation at immunohistochemistry analysis but had a minimally invasive phenotype defined at DT imaging, tumor samples were used for next-generation sequencing of rarer mutations that involved both IDH-1 and IDH-2. The tumor specimens were reviewed and DNA was extracted from tumor-rich tissue. DNA was then amplified for 207 mutational hotspot regions in 50 cancer-associated genes by using primers (Ion AmpliSeq Cancer Hotspot Panel v2; Thermo Fisher Scientific, Waltham, Mass), sequenced (Ion PGM System; Thermo Fisher Scientific), and analyzed for mutation status (Torrent Suite Software and Ion Reporter Software; Thermo Fisher Scientific). Mutations of IDH-1 on exon 4, codon 132, and mutations of IDH-2 on exon 4, codon 172, were sought because mutations at these regions account for all other IDH mutations (3).

Statistical Analysis

Data were analyzed by using statistical software (SPSS version 22; IBM, Armonk, NY), and *P* values of less than .05 indicated statistical significance. Differences in age between groups on the basis of IDH-1 mutation status were evaluated by using an independent sample *t* test. The frequency of the three different invasive phenotypes was compared according to IDH-1 R132H status by using the Freeman-Halton extension of the Fisher exact probability test for a 2 × 3 contingency table.

The diagnostic accuracy of a minimally invasive phenotype to detect the IDH-1 R132H mutation was calculated by using a 2 × 2 contingency table, with 95% confidence intervals calculated with the log method (23).

Results

Patients Studied

Seventy patients were recruited to this study. Nine of 70 patients (13%) had the IDH-1 R132H mutation (six men; median age, 45 years [range, 22.0–59.6 years]) and 61 of 70 (87%) had IDH-1 wild type (49 men; median age, 61.4 years [range, 31.4–73.0 years]). The group with the IDH-1 R132H mutation was significantly younger than the group with wild type (P = .003). The tumors with IDH-1 mutation were in the frontal lobe (six of nine) or temporal lobe (three of nine). The IDH-1 wild-type tumors were in the frontal lobe (22 of 61), temporal lobe (21 of 61), parietal lobe (11 of 61), and occipital lobe (seven of 61).

Invasive Phenotypes and IDH-1 Status

For the entire cohort, 42 of 70 (60%) tumors were diffusely invasive glioblastomas, 14 of 70 (20%) were locally invasive, and 14 of 70 (20%) were minimally invasive. Of the IDH-1 wild-type tumors, 42 of 61 (69%) were diffusively invasive glioblastomas, 14 of 61 (23%) were locally invasive, and five of 61 (8%) were minimally invasive. In all nine patients with an R132H mutation, the tumors were minimally invasive. The difference in these distributions was significant ($P < .001$).

Further sequencing in the five of 61 patients who were negative for IDH-1 R132H and who had a minimally invasive pattern revealed no rarer mutations of IDH-1 or IDH-2, which suggested that they had IDH wild-type tumors.

Minimal Invasive Phenotype Detection of IDH-1 R132H Mutation

Use of the minimally invasive phenotype as a diagnostic test for IDH mutation had sensitivity of 100% (95% confidence interval: 66.4%, 100%) and specificity of 92% (95% confidence interval: 81.9%, 97.3%).

Figure 1

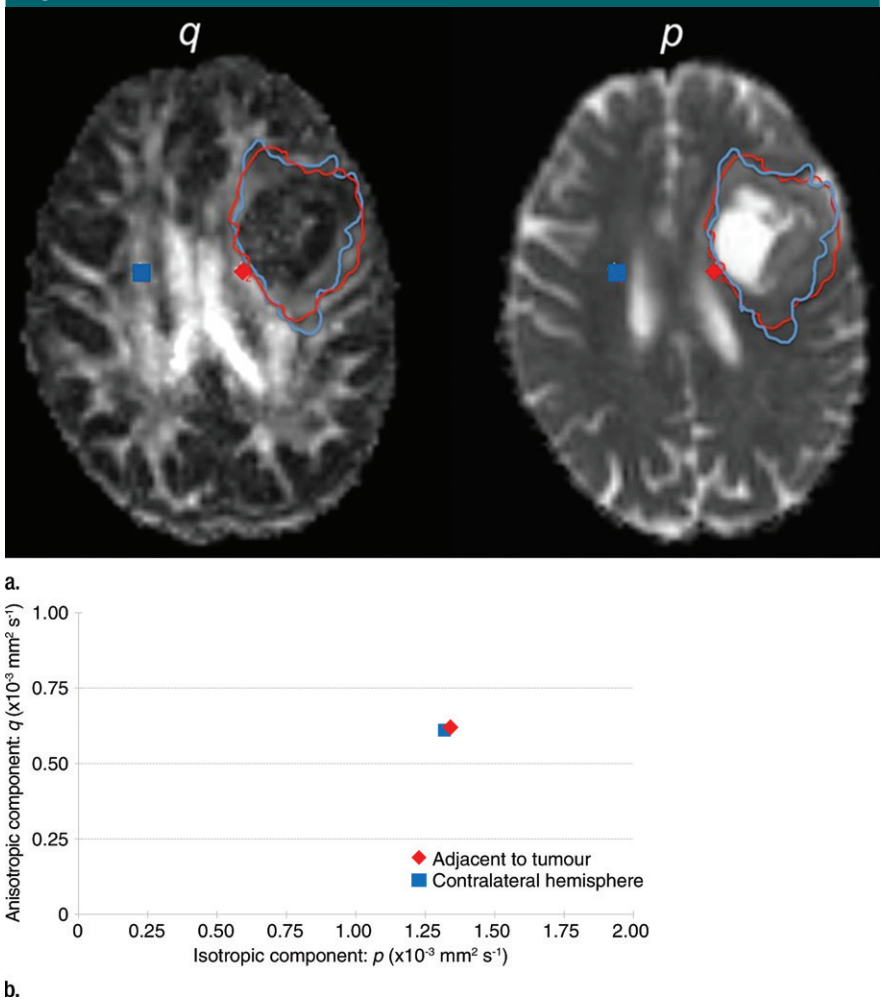

Figure 1: **(a)** Anisotropic *(q)* and isotropic *(p)* DT imaging maps in a 46-year-old man with IDH-mutated glioblastoma. The abnormality outlined within the anisotropic component (*q*, outlined by the blue line) is similar to the isotropic abnormality (*p*, outlined by the red line). The diffusion tissue signature could be measured in white matter regions of interest adjacent to the tumor (red) and in a similar location in the contralateral hemisphere (blue). **(b)** The diffusion tissue signature in adjacent white matter shows that, compared with the contralateral white matter, these values are consistent with no invasion of the white matter tract.

Discussion

Our study showed that in glioblastomas with the IDH-1 mutation, DT imaging showed features of a less invasive tumor compared with IDH-1 wild-type glioblastomas. All the IDH-1–mutated glioblastomas exhibited a minimally invasive phenotype defined at DT imaging—a phenotype previously shown to be associated with a good prognosis. Because most patients with glioblastoma will die of local tumor progression, limited local invasion may contribute to the better prognosis observed in IDH-mutated glioblastomas.

Previous studies (7,24,25) of imaging correlates of IDH-mutation status showed that IDH status leads to a different distribution in tumor location. IDH-mutated tumors are commonly located in the frontal lobe, whereas IDH

Figure 2

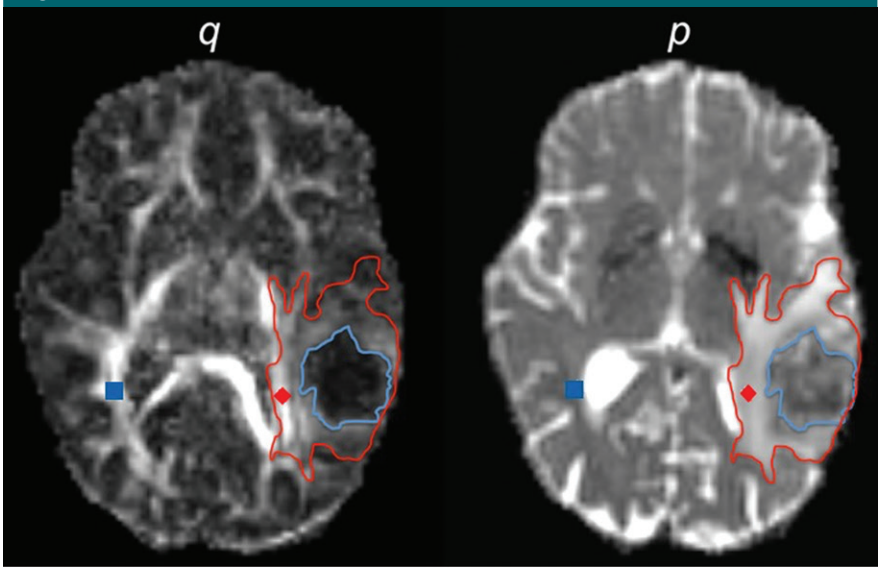

a.

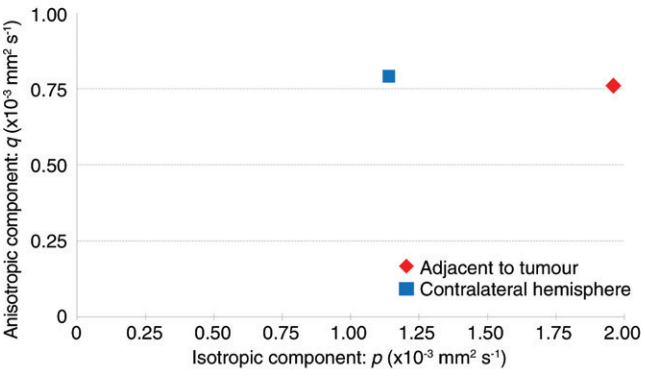

b.

Figure 2: **(a)** Anisotropic *(q)* and isotropic *(p)* DTI maps in a 59-year-old man with IDH wild-type glioblastoma. It shows that the isotropic abnormality (*p*, outlined by the red line) is larger than the anisotropic component (*q*, outlined by the blue line) in more than one direction, making it a diffuse phenotype. The diffusion tissue signature was measured in white matter regions of interest adjacent to the tumor (shown in red) and in a similar location in the contralateral hemisphere (shown in blue). **(b)** The diffusion tissue signatures confirm that there is an increase in the isotropic component *(p)* of the DT compared with the contralateral white matter, while the anisotropic component *(q)* is unchanged. This diffusion tissue signature fits tumor invasion.

wild-type gliomas are commonly found in insular regions (26). This frontal distribution may make these tumors more likely to be resectioned (7) and may also account for the improved outcome. Additionally, it may also explain why our study recruited so many patients who had tumors with a IDH-1 mutation, which were suitable for radical resection. Studies that observed the visual tumor margin provided mixed results. Some studies suggested that a distinct enhanced border is more likely to be observed in tumors with a IDH-1 mutation (26), whereas other studies found no association with IDH-1 mutation status (25). Studies that used diffusion imaging found increased apparent diffusion coefficient in the peritumoral region, which suggested reduced cellularity and angiogenesis in these regions (27). Perfusion imaging helped to confirm reduced perfusion in IDH-mutated tumors (28). This supports our finding of reduced tumor invasion in these IDH-mutated tumors.

At first glance, our results would appear to be contrary to those reported by Baldock et al (29), who found that IDH-mutated tumors were more invasive. Those investigators calculated a biologic aggressiveness ratio (the ρ/D ratio) from estimating parameters to quantify the net proliferation rate (ρ) and tumor cell dispersion or diffusion rate (D). They found that glioblastomas with a IDH-1 mutation have a low ρ/D ratio, which suggests markedly dispersed tumor cells with a low central density of tumor cells. This may explain the postmortem finding of dispersed R132H-positive cells throughout the brain (30). In reality, imaging methods can depict only a high density of tumor cells. Biopsy studies have confirmed that within the isotropic (p) abnormality there was high density of tumor cells, with undetectable tumor cells outside of this region (10). Our findings show low tumor cell density in the immediate peritumoral region, a finding that agrees with mathematical modeling from Baldock et al. Newer diffusion techniques, such as restriction spectrum imaging, that can differentiate restricted from hindered diffusion (31) may better reflect tumor cellularity in this peritumoral area.

The fact that the invasive margin of glioblastomas with IDH-1 mutation has lower cellular density might explain the improved outcome with extended resection beyond the contrast agent–enhanced tumor into the unenhanced fluid-attenuated inversion recovery abnormality (7). Although this study failed to show a similar outcome in IDH wild-type tumors, recent studies provide some evidence that resection into noncontrast-enhanced tumor does improve outcome (32). We conclude that in the absence of better imaging techniques to distinguish between tumor and cerebral edema, extending resection into the fluid-attenuated inversion recovery region improves survival without substantial postoperative morbidity. Our DT imaging method might provide a better target for resection into the

nonenhanced tumor, and we could postulate that patients with limited invasion with IDH wild-type glioblastomas may have a better outcome with more extensive resection. In other words, the invasive phenotype, rather than the IDH mutation status, may account for improved outcome with extended surgery.

One major issue is to understand the mechanism of reduced invasiveness with IDH mutations. Studies of glioma cells with IDH-2 mutation show upregulation of hypoxia-inducible factor-1α and β-catenin (33), which leads to increased secretion of metalloproteinases (34). This promotes glioma cell invasion, without the need for hypoxia to induce these hypoxia-inducible factor-1α mechanisms. This may explain the increase in low cell density invasion but less gross invasion.

A limitation of our study is that our data are derived from a relatively small number of IDH-mutated glioblastomas. These mutations are rare: they occur in approximately 10% of all glioblastomas and only 4.8% of all primary glioblastomas (3). Thus, it will be difficult to have sufficient numbers outside of large cohorts. Because the results within our small series were so different from those observed in IDH wild-type tumors, we believe that we have shown a true difference in tumor biology. In addition, because we used only immunohistochemistry to identify the most common IDH-1 mutation in most of our patients, we may have missed some of the rarer mutations of IDH-1 and IDH-2. For a small group with minimally invasive phenotype, we were able to use pyrosequencing for these rarer mutations and confirm that this cohort had no additional IDH mutations. Although immunohistochemistry for R132H will correctly determine the IDH mutation status in 88%–99% of tumors (35), data from Zou et al (35) suggest that immunohistochemistry has an overall accuracy of 94% compared with sequencing. If we assume that 6% of our remaining patients have IDH mutations, then we would have missed approximately four patients. With use of these data, our diagnostic accuracy would retain a high specificity (91%) and sensitivity (70%).

In conclusion, we used DT imaging to study the invasive properties of the invasive margin of glioblastomas and have shown that glioblastomas with IDH-1 mutation exhibit a minimally invasive DT imaging–defined phenotype. This finding may help to explain the good prognosis of this group of tumors and it supports the role of more extensive local therapy for these tumors.

Disclosures of Conflicts of Interest: S.J.P. disclosed no relevant relationships. **K.A.** disclosed no relevant relationships. **H.L.** disclosed no relevant relationships. **N.R.B.** disclosed no relevant relationships. **J.L.Y.** disclosed no relevant relationships. **V.C.L.** disclosed no relevant relationships. **T.J.L.** disclosed no relevant relationships.

References

1. Watanabe T, Nobusawa S, Kleihues P, Ohgaki H. IDH1 mutations are early events in the development of astrocytomas and oligodendrogliomas. Am J Pathol 2009;174(4):1149–1153.
2. Parsons DW, Jones S, Zhang X, et al. An integrated genomic analysis of human glioblastoma multiforme. Science 2008;321(5897):1807–1812.
3. Yan H, Parsons DW, Jin G, et al. IDH1 and IDH2 mutations in gliomas. N Engl J Med 2009;360(8):765–773.
4. Verhaak RG, Hoadley KA, Purdom E, et al. Integrated genomic analysis identifies clinically relevant subtypes of glioblastoma characterized by abnormalities in PDGFRA, IDH1, EGFR, and NF1. Cancer Cell 2010;17(1):98–110.
5. Capper D, Weissert S, Balss J, et al. Characterization of R132H mutation-specific IDH1 antibody binding in brain tumors. Brain Pathol 2010;20(1):245–254.
6. Eckel-Passow JE, Lachance DH, Molinaro AM, et al. Glioma groups based on 1p/19q, IDH, and TERT promoter mutations in tumors. N Engl J Med 2015;372(26):2499–2508.
7. Beiko J, Suki D, Hess KR, et al. IDH1 mutant malignant astrocytomas are more amenable to surgical resection and have a survival benefit associated with maximal surgical resection. Neuro-oncol 2014;16(1):81–91.
8. Lunsford LD, Martinez AJ, Latchaw RE. Magnetic resonance imaging does not define tumor boundaries. Acta Radiol Suppl 1986;369:154–156.
9. Kelly PJ, Daumas-Duport C, Kispert DB, Kall BA, Scheithauer BW, Illig JJ. Imaging-based stereotaxic serial biopsies in untreated intracranial glial neoplasms. J Neurosurg 1987;66(6):865–874.
10. Price SJ, Jena R, Burnet NG, et al. Improved delineation of glioma margins and regions of infiltration with the use of diffusion tensor imaging: an image-guided biopsy study. AJNR Am J Neuroradiol 2006;27(9):1969–1974.
11. Price SJ, Burnet NG, Donovan T, et al. Diffusion tensor imaging of brain tumours at 3T: a potential tool for assessing white matter tract invasion? Clin Radiol 2003;58(6):455–462.
12. Provenzale JM, McGraw P, Mhatre P, Guo AC, Delong D. Peritumoral brain regions in gliomas and meningiomas: investigation with isotropic diffusion-weighted MR imaging and diffusion-tensor MR imaging. Radiology 2004;232(2):451–460.
13. Castellano A, Donativi M, Bello L, et al. Evaluation of changes in gliomas structural features after chemotherapy using DTI-based functional diffusion maps (fDMs): A preliminary study with intraoperative correlation [abstr]. In: Proceedings of the Nineteenth Meeting of the International Society for Magnetic Resonance in Medicine. Berkeley, Calif: International Society for Magnetic Resonance in Medicine, 2011; 2411.
14. Price SJ, Jena R, Burnet NG, Carpenter TA, Pickard JD, Gillard JH. Predicting patterns of glioma recurrence using diffusion tensor imaging. Eur Radiol 2007;17(7):1675–1684.
15. Price SJ, Young AM, Scotton WJ, et al. Multimodal MRI can identify perfusion and metabolic changes in the invasive margin of glioblastomas. J Magn Reson Imaging 2016;43(2):487–494.
16. Mohsen LA, Shi V, Jena R, Gillard JH, Price SJ. Diffusion tensor invasive phenotypes can predict progression-free survival in glioblastomas. Br J Neurosurg 2013;27(4):436–441.
17. Stummer W, Pichlmeier U, Meinel T, et al. Fluorescence-guided surgery with 5-aminolevulinic acid for resection of malignant glioma: a randomised controlled multicentre phase III trial. Lancet Oncol 2006;7(5):392–401.
18. Peña A, Green HA, Carpenter TA, Price SJ, Pickard JD, Gillard JH. Enhanced visualization and quantification of magnetic resonance diffusion tensor imaging using the p:q tensor decomposition. Br J Radiol 2006;79(938):101–109.

19. Scherer HJ. The forms of growth in gliomas and their practical significance. Brain 1940;63(1):1–35.

20. Burger PC, Heinz ER, Shibata T, Kleihues P. Topographic anatomy and CT correlations in the untreated glioblastoma multiforme. J Neurosurg 1988;68(5):698–704.

21. Price SJ, Peña A, Burnet NG, et al. Tissue signature characterisation of diffusion tensor abnormalities in cerebral gliomas. Eur Radiol 2004;14(10):1909–1917.

22. Louis DN, Ohgaki H, Wiestler OD, Cavenee WK. WHO Classification of Tumours of the Central Nervous System. Lyon, France: IARC, 2007.

23. Altman DG, Machin D, Bryant TN, Gardner MJ, eds. Statistics with confidence. 2nd ed. London, England: BMJ Books, 2000.

24. Carrillo JA, Lai A, Nghiemphu PL, et al. Relationship between tumor enhancement, edema, IDH1 mutational status, MGMT promoter methylation, and survival in glioblastoma. AJNR Am J Neuroradiol 2012;33(7):1349–1355.

25. Sonoda Y, Shibahara I, Kawaguchi T, et al. Association between molecular alterations and tumor location and MRI characteristics in anaplastic gliomas. Brain Tumor Pathol 2015;32(2):99–104.

26. Metellus P, Coulibaly B, Colin C, et al. Absence of IDH mutation identifies a novel radiologic and molecular subtype of WHO grade II gliomas with dismal prognosis. Acta Neuropathol (Berl) 2010;120(6):719–729.

27. Tan WL, Huang WY, Yin B, Xiong J, Wu JS, Geng DY. Can diffusion tensor imaging noninvasively detect IDH1 gene mutations in astrogliomas? A retrospective study of 112 cases. AJNR Am J Neuroradiol 2014;35(5):920–927.

28. Kickingereder P, Sahm F, Radbruch A, et al. IDH mutation status is associated with a distinct hypoxia/angiogenesis transcriptome signature which is non-invasively predictable with rCBV imaging in human glioma. Sci Rep 2015;5:16238.

29. Baldock AL, Yagle K, Born DE, et al. Invasion and proliferation kinetics in enhancing gliomas predict IDH1 mutation status. Neuro-oncol 2014;16(6):779–786.

30. Sabit H, Nakada M, Furuta T, et al. Characterizing invading glioma cells based on IDH1-R132H and Ki-67 immunofluorescence. Brain Tumor Pathol 2014;31(4):242–246.

31. McDonald CR, White NS, Farid N, et al. Recovery of white matter tracts in regions of peritumoral FLAIR hyperintensity with use of restriction spectrum imaging. AJNR Am J Neuroradiol 2013;34(6):1157–1163.

32. Li YM, Suki D, Hess K, Sawaya R. The influence of maximum safe resection of glioblastoma on survival in 1229 patients: Can we do better than gross-total resection? J Neurosurg 2016;124(4):977–988.

33. Fu Y, Zheng S, Zheng Y, et al. Glioma derived isocitrate dehydrogenase-2 mutations induced up-regulation of HIF-1α and β-catenin signaling: possible impact on glioma cell metastasis and chemo-resistance. Int J Biochem Cell Biol 2012;44(5):770–775.

34. Fu Y, Zheng Y, Li K, et al. Mutations in isocitrate dehydrogenase 2 accelerate glioma cell migration via matrix metalloproteinase-2 and 9. Biotechnol Lett 2012;34(3):441–446.

35. Zou Y, Bai HX, Wang Z, Yang L. Comparison of immunohistochemistry and DNA sequencing for the detection of IDH1 mutations in gliomas. Neuro-oncol 2015;17(3):477–478.